Optimal Spectrum Utilization in Joint Automotive Radar and Communication Networks

You Han*, Eylem Ekici*
*Department of Electrical and Computer Engineering
The Ohio State University, Columbus, Ohio 43210
Email: han.639@osu.edu, ekici@ece.osu.edu

Haris Kremo†, Onur Altintas †
†Toyota InfoTechnology Center Co., Ltd, Tokyo, Japan
Email: {hkremo, onur}@jp.toyota-itc.com

***Abstract*—Due to rapid growth of wireless traffic demands in vehicular networks, spectrum scarcity is becoming urgent in the Dedicated Short Range Communication (DSRC) band. One solution is reusing automotive radar bands without degrading radar performance. Despite having massive bandwidths, imaging accuracy of automotive radars is still low due to correlations between sequential target observations of single radar. A solution is that vehicles exchange imaging information through vehicle-to-vehicle communications. Since observations of different vehicles are less correlated, Joint Automotive Radar and Communication (JARC) network is able to improve imaging accuracy. More importantly, some spectrum resources can be left to alleviate the DSRC spectrum scarcity problem. In this paper, we derive the Cramer-Rao bound for parameter estimation in JARC networks. Then, we formulate the spectrum utilization problem as an NP-complete integer quadratic program, to which we propose an optimal (in expectation) algorithm with low complexity. Finally, efficacy of the algorithm is illustrated through numerical results.**

I. Introduction

Due to rapid increase of wireless traffic demands in vehicular networks, many studies have suggested that the spectrum scarcity problem in the 5.9 GHz Dedicated Short Range Communications (DSRC) band is becoming more urgent [1]. Meanwhile, massive frequency bands have been allocated to automotive radars in the 24/26 GHz UWB and 77 GHz band in many countries. However, imaging accuracy of automotive radars is still low due to correlations between sequential target observations of single radar, and thus the radar bands can be considered underutilized. Hence, joint automotive radar and communication (JARC) networks were proposed to incorporate vehicle-to-vehicle (V2V) communications in automotive radars to improve efficiency of the radar bands [2] [3].

Since some of the radar imaging time is allocated to vehicular communications, one concern is that RI accuracy can be degraded. In fact, the interaction between RI and V2V communications is not a zero-sum game: RI can benefit from V2V communications because neighboring vehicles can improve RI accuracy by sharing RI results. Specifically, instead of using its own temporally correlated radar observations, each vehicle can utilize observations with low spatial correlation from its neighbors to improve its RI accuracy. V2V communications can also benefit from RI because RI helps a vehicle identify and locate its receivers. Furthermore, RI can help V2V communications establish directional V2V links and beamforming (e.g., 5G community is looking into tracking of mobile devices in millimeter wave bands). Moreover, radar signals can be used to carry control information for V2V communications, and communication signals can also be used as radar pulses [3]. More importantly, since V2V communications can improve RI accuracy, some radar spectrum resources can be left for other vehicular communications after baseline RI accuracy requirements are satisfied, which alleviates the spectrum scarcity problem in the DSRC band.

Although JARC networks have been implemented in several existing works [2] [3], to the best of our knowledge, no works have provided a theoretical analysis on performance of the JARC network. In this paper, we try to fill this gap by presenting a theoretical study of the JARC networks. Contributions of our work are threefold:

1) We study the tradeoff between radar imaging and V2V communications, and derive Cramer-Rao lower bound (CRLB) for cooperative parameter estimation in the JARC network.
2) We formulate the spectrum utilization problem as an integer quadratic program (IQP) with the objective of maximizing remaining spectrum resources for other vehicular communications subject to radar imaging accuracy requirements.
3) To solve the formulated NP-complete problem, we devise a quadratic programming-based method associated with an integer rounding algorithm. The method is optimal in expectation, which means that our solution achieves the optimal value of the relaxed IQP in expectation at the cost of relaxing some constraints.

The remainder of this paper is organized as follows. We present the study of tradeoff between RI and V2V communications and CRLB derivation in Section II. Then, the system model and problem formulation are described in Section III. In Section IV, we discuss the proposed method. Numerical results are presented in Section V, followed by the conclusion in Section VI.

II. Tradeoff of Radar Imaging and V2V Communications

In this section, we characterize RI accuracy in the JARC network using estimation theory. As shown in Figure 1, in a pure automotive radar network, each vehicle tracks a target by transmitting radar signals every T_r milliseconds within a period T. In the JARC network, each vehicle spends part of the

978-1-5090-1311-1/16/$31.00 ©2016 IEEE

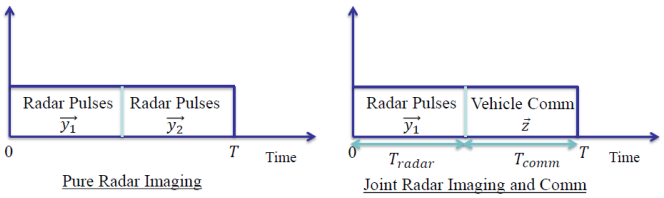

Figure 1. Time allocation in the pure radar and JARC networks

time on tracking the target by itself, and exchanges tracking information with its neighbors in the remaining time. In both networks, each vehicle estimates parameters (e.g., location and velocity) of the target at the end of every tracking period.

As shown in Figure 1, let T_{radar} and T_{comm} be the RI and communication time, respectively, and $T = T_{radar} + T_{comm}$ be the tracking period. Let X be the target parameter to be estimated by all vehicles. In this paper, X is assumed to be an unknown constant parameter. Let Y_j be the estimated value of X based on the j-th reflected radar signal. Since the RI rate is very high (e.g., 1000 signals per second), two sequential estimations Y_j and Y_{j-1} are assumed to be linearly correlated. Therefore, we can obtain the following correlation equations at vehicle i:

$$\begin{aligned} Y_1 &= X + N_{i1}, \\ Y_2 &= \alpha Y_1 + (1-\alpha)X + N_{i2}, \\ &\cdots \\ Y_j &= \alpha Y_{j-1} + (1-\alpha)X + N_{ij}, \end{aligned} \tag{1}$$

where α is a constant factor characterizing the linear correlation between two sequential observations, and $N_{ij} \sim \mathcal{N}(0, \sigma_i^2), \forall j$ are i.i.d estimation errors at vehicle i. The assumption that estimation errors follow Gaussian distribution has been justified in both [4] (Page 301, Chapter 10) and [5] (Page 322). In addition, X and $N_{ij}, \forall j$ are assumed to be independent. From Equation (1), we can see that $\{Y_1, Y_2 \cdots\}$ forms a Markov chain.

Suppose every vehicle communicates with K neighbors. As shown in Figure 1, let $\overrightarrow{y_1}$ and $\overrightarrow{y_2}$ be the observed parameter sequences by a vehicle in the pure radar network. In contrast, let $\overrightarrow{z}$ be the observed parameter sequences from neighbors of the vehicle. Specifically, the three vectors are defined as

$$\begin{aligned} &\overrightarrow{y_1} = (Y_1, Y_2, \cdots Y_m), \overrightarrow{y_2} = (Y_{m+1}, Y_{m+2}, \cdots Y_{m+n}), \\ &\overrightarrow{z} = (\overrightarrow{Z_1}, \overrightarrow{Z_2}, \cdots \overrightarrow{Z_K}), \end{aligned} \tag{2}$$

where m and n denote the number of transmitted signals in $\overrightarrow{y_1}$ and $\overrightarrow{y_2}$, respectively, and $\overrightarrow{Z_i} = (Y_1^i, Y_2^i, \cdots Y_{m_i}^i)$ denotes observed parameter sequences from the i-th neighbor. In addition, observed parameter sequences from different vehicles (i.e., $\overrightarrow{y_1}, \overrightarrow{Z_1}, \overrightarrow{Z_2} \cdots \overrightarrow{Z_K}$) are assumed to be independent.

The assumption of temporal correlation between sequential radar observations has been widely used in the literature (e.g., [6], [7]). Specifically, two sequential measurements are correlated because round trip time of signals is usually so small such that time difference between two observations is rather small. Since wireless environment cannot change significantly and the vehicle cannot move far during such short time, the two observations are very likely to be correlated. The assumption of independent observations at different vehicles is due to different imaging environment at these vehicles, e.g., line-of-sight path to the target, local interference, radar hardware, thermal noise, and nearby obstacles etc.

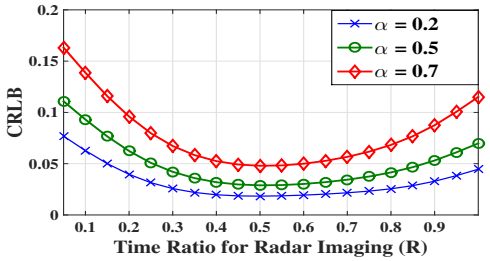

Figure 2. An example of CRLB values in a JARC network

Next, we analyze radar performance in the JARC network using estimation theory. Since X is an unknown constant parameter, Maximum Likelihood (ML) estimators can be used to estimate X. Since usually no closed form equations exist for Mean Squared Error (MSE) of the ML estimators, performance of the estimators is often evaluated by calculating lower bound of the MSE (i.e., CRLB). However, we show that there exists a valid "efficient" ML estimator whose MSE reaches the CRLB.

In the JARC network, each vehicle estimates target parameters using its own observations $\overrightarrow{y_1}$ and observations of its neighbors $\overrightarrow{z}$. We first derive the likelihood function of the observations in Equation (3), where y_j^i is a realization of Y_j^i, the second equation is due to independence of $\overrightarrow{y_1}, \overrightarrow{z_1}, \overrightarrow{z_2}, \cdots \overrightarrow{z_K}$, and the third equation is due to Markovian property of the $\{Y_1, Y_2 \cdots\}$ sequences. Next, we compute the Fisher Information of X as

$$\begin{aligned} I(X) &= -\mathrm{E}\left[\frac{\partial^2}{\partial X^2} \log p(\overrightarrow{y_1}, \overrightarrow{z}|X)\right] \\ &= \sum_{i=0}^{K} \frac{1 + (m_i - 1)(1-\alpha)}{\sigma_i^2}. \end{aligned} \tag{4}$$

Assume the efficient estimator exists, which is calculated as

$$\begin{aligned} &\hat{X}_{eff}(\overrightarrow{y_1}, \overrightarrow{z}) = X + \frac{1}{I(X)} \frac{\partial}{\partial X} \log p(\overrightarrow{y_1}, \overrightarrow{z}|X) \\ &= X + \frac{1}{I(X)} \frac{y_1 - X + \sum_{j=2}^{m_0}(y_j - \alpha y_{j-1} - (1-\alpha)X)}{\sigma_0^2} \\ &+ \frac{1}{I(X)} \sum_{i=1}^{K} \frac{(y_1^i - X + \sum_{j=2}^{m_i}(y_j^i - \alpha y_{j-1}^i - (1-\alpha)X))}{\sigma_i^2} \\ &= X - X + \frac{1}{I(X)} \sum_{i=0}^{K} \frac{y_1^i + \sum_{j=2}^{m_i}(y_j^i - \alpha y_{j-1}^i)}{\sigma_i^2} \\ &= \frac{\sum_{i=0}^{K} \left[y_1^i + \sum_{j=2}^{m_i}(y_j^i - \alpha y_{j-1}^i)\right] / \sigma_i^2}{\sum_{i=0}^{K} \left[1 + (m_i - 1)(1-\alpha)\right] / \sigma_i^2}. \end{aligned} \tag{5}$$

Since $\hat{X}_{eff}(\overrightarrow{y_1}, \overrightarrow{z})$ is not a function of X, it is a valid and efficient estimator. Therefore, its CRLB is also its MSE:

$$CRLB = \frac{1}{I(X)} = 1 / \sum_{i=0}^{K} \frac{1 + (m_i - 1)(1-\alpha)}{\sigma_i^2}. \tag{6}$$

$$p(\overrightarrow{y_1}, \overrightarrow{z}|X) = p(\overrightarrow{y_1}, \overrightarrow{z_1}, \cdots \overrightarrow{z_K}|X) = p(\overrightarrow{y_1}|X)\prod_{i=1}^{K} p(\overrightarrow{z_i}|X) = p(Y_1|X)\prod_{j=2}^{m_i} p(Y_j|Y_{j-1}, X)\prod_{i=1}^{K}\left(p(Y_1^i|X)\prod_{j=2}^{m_i} p(Y_j^i|Y_{j-1}^i, X)\right)$$

$$= \left(\frac{1}{\sqrt{2\pi\sigma_0^2}}\right)^{m_0} \exp\left(-\frac{(y_1 - X)^2}{2\sigma_0^2}\right)\prod_{j=2}^{m_0}\exp\left(-\frac{(y_j - \alpha y_{j-1} - (1-\alpha)X)^2}{2\sigma_0^2}\right)$$

$$\cdot \prod_{i=1}^{K}\left[\left(\frac{1}{\sqrt{2\pi\sigma_i^2}}\right)^{m_i} \exp\left(-\frac{(y_1^i - X)^2}{2\sigma_i^2}\right)\prod_{j=2}^{m_i}\exp\left(-\frac{(y_j^i - \alpha y_{j-1}^i - (1-\alpha)X)^2}{2\sigma_i^2}\right)\right]. \tag{3}$$

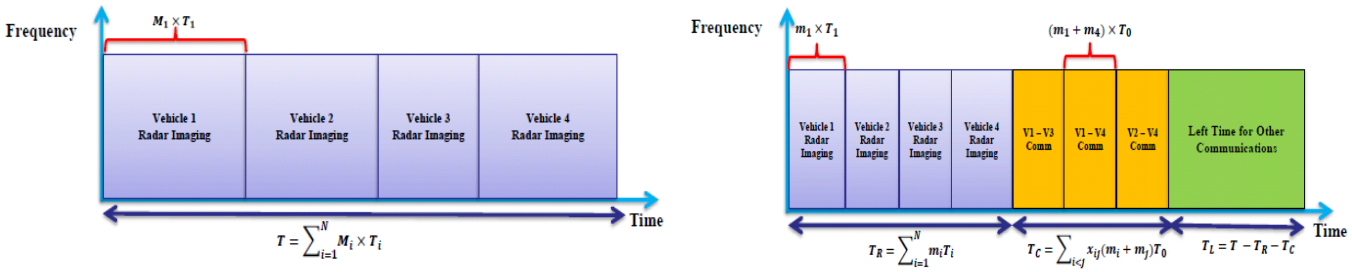

(a) Scheduling in a pure automotive radar network

(b) Scheduling in a JARC network

Figure 3. Spectrum usage in pure automotive radar network and JARC network

Next, we show that the JARC network is able to improve the RI accuracy. Specifically, we consider a JARC network in which all vehicles allocate the same ratio of time to RI. In Figure 1, let $R = T_{radar}/T$ be the time ratio allocated to RI, and T_r, T_c be the time needed for a single radar signal transmission and a single V2V communication session. We set $T_r = 7.33$ microseconds, and $T = 128T_r$. In addition, it is assumed that each V2V session takes $T_c = 15T_r$. Moreover, we set the variance of noise $\sigma_i^2 = 5$ dB, $\forall i$. We consider three different scenarios with small ($\alpha = 0.2$), medium ($\alpha = 0.5$) and large ($\alpha = 0.7$) temporal correlation levels. Given this setup, the corresponding MSE (CRLB) is shown in Figure 2.

Figure 2 shows that, compared with the pure automotive radar network (i.e., RI time ratio $R = 1$), the JARC network is able to achieve higher RI accuracy (i.e., lower CRLB values). Therefore, if we use the CRLB value in the pure automotive radar network as a baseline requirement in the JARC network, certain amount of time ratio can be left for other vehicular communications after the baseline CRLB is achieved.

III. System Model and Problem Formulation

In this section, we study the spectrum utilization problem in the JARC network, where a master vehicle makes spectrum allocation decisions at the beginning of every scheduling period. As shown in Figure 3, let T_i be the round-trip time between vehicle i (denoted by V_i) and the target, and M_i be the number of radar signals V_i transmits in order to achieve its RI accuracy in the pure automotive radar network.

Parameters used in the following problem formulation can be obtained as follows. First, we assume that the scheduling/tracking period T is a known constant that is determined by safety requirements of automotive radars, and T_i at each period can be calculated using distance, angle, and relative velocity information in its previous period. Given T and $T_i, \forall i$, we assume that M_i values in the pure automotive radar network can be obtained by considering CRLB requirements of cooperating vehicles. In other words, our spectrum utilization optimization is performed based on a known radar imaging scheduling (i.e., M_i values) in the pure automotive radar network. Moreover, since variance of estimation errors (i.e., σ_i^2 values) are determined by factors like local noise, thermal noise and nearby obstacles etc, they change slowly and thus are assumed known and periodically updated by each vehicle.

In this paper, scheduling decisions are: (1) $m_i \geq 1, \forall i$: the number of radar pulses each vehicle i should transmit; (2) $x_{ij} \in \{0, 1\}, \forall i, j$: whether V_i and V_j should exchange imaging results. In particular, we can see that $x_{ij} = x_{ji}, \forall (i, j)$, and $x_{ii} = 0, \forall i$, because vehicles do not communicate with themselves. After the decision parameters are determined by the master vehicle, they are broadcast to all cooperating vehicles on a reliable JARC control channel using omnidirectional radios. Ideally, we would like to have a distributed system, but as an initial step we assume centralized allocation. Moreover, m_i is required to be at least 1 in case some V2V links fail due to unexpected obstacles.

Let N be the number of vehicles in the JARC network, and we continue to study communication overhead for exchanging RI information between two vehicles V_i and V_j. Since directional antennas are used in automotive radars, a vehicle may not be able to broadcast its RI information to all its neighbors through radars. Hence, it has to communicate with its

neighbors one-by-one. Moreover, the amount of information V_i needs to transmit to V_j is proportional to the number of radar signals it has transmitted (i.e., m_i in Equation (5)). Therefore, the time needed for V_i and V_j to exchange RI information is $(m_i + m_j) \times T_0$, where T_0 is the time needed to transmit one unit of information. Furthermore, as shown in Figure 3, the remaining time for other vehicular communications is

$$\begin{aligned} T_L &= T - T_R - T_C \\ &= T - \sum_{i=1}^{N} m_i T_i - \sum_{\forall(i,j):i<j} x_{ij}(m_i + m_j)T_0 \\ &= T - \sum_{i=1}^{N} m_i T_i - \frac{1}{2} \sum_{\forall(i,j)} x_{ij}(m_i + m_j)T_0 \\ &= T - \sum_{i=1}^{N} m_i T_i - \frac{1}{2} \left(\sum_{\forall(i,j)} x_{ij} m_i T_0 + \sum_{\forall(i,j)} x_{ij} m_j T_0 \right) \\ &= T - \sum_{i=1}^{N} m_i T_i - \sum_{\forall(i,j)} x_{ij} m_i T_0 \\ &= T - \sum_{i=1}^{N} m_i \left(T_i + \sum_{j=1}^{N} x_{ij} T_0 \right), \end{aligned} \tag{7}$$

where $T = \sum_{i=1}^{N} M_i T_i$ is the scheduling period, T_R is the total RI time, T_C is the total V2V communication time for exchanging radar imaging results, and the fifth equality is due to $x_{ij} = x_{ji}, \forall(i,j)$. Let $\mathbf{m}^T = [m_1, m_2 \cdots m_N]$ and $X = \{x_{ij} \in \{0,1\}, \forall i,j\}$ be the decision variables, and the JARC spectrum utilization problem can be formulated as

$$\begin{aligned} \max_{X, \mathbf{m} \in \mathbb{Z}^+} \; & T_L \\ \text{s.t. } & C1 : CRLB_i(\mathbf{m}, X) \le \beta_i, \forall i \in \{1, 2 \cdots N\}, \\ & C2 : T_L \ge 0, \\ & C3 : x_{ij} \le C_{ij}, \forall i \ne j, \\ & C4 : x_{ij} = x_{ji}, \forall i < j, \end{aligned} \tag{P.1}$$

where $CRLB_i(\mathbf{m}, X) = \frac{1}{I_i(\mathbf{m}, X)}$, $I_i(\mathbf{m}, X) = \frac{1+(m_i-1)(1-\alpha)}{\sigma_i^2} + \sum_{j(j \ne i)} x_{ij} \frac{1+(m_j-1)(1-\alpha)}{\sigma_j^2}$ according to Equation (6), $C1$ means the CRLB of vehicle i must not be greater than a threshold β_i, $C2$ means that the maximum remaining time must be non-negative, $C3$ is communication feasibility constraint, and $C4$ is assignment constraint. In particular, $C_{ij} \in \{0,1\}$ denotes whether vehicle i and j can communicate with each other due to factors like distance, antenna direction and obstacles between them.

We continue to show that $C2$ can be removed by setting β_i values to be CRLB values in the pure radar network. Specifically, as shown in Figure 3, let $\mathbf{M} = \{M_1, M_2, \cdots M_N\}$ be a known RI scheduling in the pure radar network, and $CRLB_i(M_i) = \frac{\sigma_i}{1+(M_i+1)(1-\alpha)}$ be the corresponding CRLB of V_i. Then, we show that (P.1) can be converted to the following (P.2) by proving Lemma III.1.

$$\begin{aligned} \min_{X, \mathbf{m} \in \mathbb{Z}^+} \; & \sum_{i=1}^{N} m_i \left(T_i + \sum_{j=1}^{N} x_{ij} T_0 \right) \\ \text{s.t. } & C1 : \frac{1+(m_i-1)(1-\alpha)}{\sigma_i^2} + \sum_{j=1}^{N} x_{ij} \frac{1+(m_j-1)(1-\alpha)}{\sigma_j^2} \\ & \ge \frac{1+(M_i-1)(1-\alpha)}{\sigma_i^2}, \forall i \in \{1, 2 \cdots N\}, \\ & C2 : x_{ij} \le C_{ij}, \forall i \ne j, \\ & C3 : x_{ij} = x_{ji}, \forall i < j, \end{aligned} \tag{P.2}$$

Lemma III.1. *Problem (P.1) is equivalent to problem (P.2) when $\beta_i = CRLB_i(M_i)$.*

Proof. Firstly, instead of maximizing the remaining time (i.e., T_L in Figure 3) as in (P.1), (P.2) minimizes the total RI and imaging results sharing time (i.e., $T_R + T_C$). Then, we need to prove optimal solution of (P.2) is guaranteed to satisfy $C2$ of (P.1). The fundamental proof idea is that all CRLB constraints can be easily satisfied if no V2V communication is used.

Specifically, by setting $\beta_i = CRLB_i(M_i)$, $C1$ in (P.1) can be transformed to $C1$ in (P.2). In addition, to show that the optimal solution of (P.2) satisfies $C2$ in (P.1), we only need to find a feasible solution of (P.2) that satisfies $C2$ in (P.1). In fact, $\mathbf{m} = \mathbf{M}, x_{ij} = 0, \forall(i,j)$ is a feasible solution to (P.2), and its corresponding total RI and V2V communication time is exactly T (i.e., $T_L = T - T_R - T_C = 0$). Hence, the optimal solution of (P.2) must be able to achieve a total RI and imaging results sharing time less than or equal to T. Therefore, $C2$ of (P.1) still holds, and thus (P.2) is equivalent to (P.1). ■

IV. Quadratic Programming based Method

We can see that (P.2) belongs to integer quadratic programs, which are generally NP-complete [8]. In this section, we propose a probabilistic algorithm to (P.2) based on quadratic programming (QP), which is guaranteed to obtain an integer solution whose expectation achieves the optimum of the (P.2) and satisfies all constraints. Although the final integer solution can violate some CRLB constraints, we prove that the worst case violation is bounded. The QP-based algorithm works as follows. Firstly, we remove all integer constraints of (P.2), and thus it reduces to a QP problem with real number variables. After obtaining a fractional solution to the new QP problem, we round it into an integer solution with the aforementioned guarantees. Since numerical algorithms have been widely utilized to solve QP problems (e.g., interior-point, sequential quadratic programming and trust-region-reflective), discussions of these algorithms are omitted here. Instead, let $(\mathbf{m}^*, X^*)$ be the optimal fractional solution to the new QP problem, we convert it into an integer solution $(\mathbf{m}, X)$.

Integer rounding algorithms can be generally classified into two categories: dependent and independent ones. Dependent rounding algorithms consider interactions between rounding correlated variables, while independent rounding algorithms

round every fractional variable without considering its impact on other variables. Since the dependent rounding usually has theoretical performance guarantees in both achieved utility and constraint violations while the independent rounding only has guarantee in the achieved utility, the dependent rounding is always preferred. However, the dependent rounding idea only applies to assignment variables [9]. Therefore, in this section, we first design a dependent rounding algorithm for assignment variables X^* to achieve guaranteed performance in both utility and constraint violations, and then design an independent rounding algorithm for RI scheduling variables $\mathbf{m}^*$ to achieve only guaranteed utility performance.

A. Rounding Algorithm for X^*

The dependent rounding algorithm discussed in [9] iteratively rounds all fractional variables into binary values without violating constraints $A\mathbf{x} \leq \mathbf{b}$. The rounding idea in a single iteration is as follows. Suppose at iteration t, after removing binary values, we are given an n-dimensional fractional solution $\mathbf{x}(t)$ that satisfies the following constraints:

1) regular tight (i.e., equality) constraints: $A_1\mathbf{x}(t) = \mathbf{b_1}$, where $A_1 \in \mathbb{R}^{m_1 \times n}, \mathbf{b_1} \in \mathbb{R}^{m_1}$,
2) regular untight (i.e., inequality) constraints: $A_2\mathbf{x}(t) < \mathbf{b_2}$, where $A_2 \in \mathbb{R}^{m_2 \times n}, \mathbf{b_2} \in \mathbb{R}^{m_2}$,
3) domain constraints: $\mathbf{x}(t) \in (0,1)^n$.

Then, a new solution $\mathbf{x}(t+1)$ is found such that

1) $E[\mathbf{x}(t+1)] = E[\mathbf{x}(t)]$,
2) tight constraints are still satisfied, i.e., $A_1\mathbf{x}(t+1) = \mathbf{b_1}$,
3) at least one entry of $\mathbf{x}(t)$ is rounded into a binary value or at least one regular untight constraint becomes tight.

The three guarantees are accomplished as follows. Firstly, assume that null space of A_1 is nontrivial, and thus $S = \{\mathbf{s} \in \mathbb{R}^n | A_1\mathbf{s} = \mathbf{0}\}$ contains at least one nonzero element. Then, randomly choose one nonzero vector from S, e.g., $\mathbf{s} \in S, \mathbf{s} \neq \mathbf{0}$. Afterwards, find positive scalar θ_1 such that

- all entries of $\mathbf{x}(t) + \theta_1\mathbf{s}$ lie in $[0,1]$,
- at least one entry of $\mathbf{x}(t) + \theta_1\mathbf{s}$ becomes integer or at least one entry of $A_2(\mathbf{x}(t) + \theta_1\mathbf{s}) - \mathbf{b_2}$ becomes zero.

Similarly, we can find another positive scalar θ_2 such that

- all entries of $\mathbf{x}(t) - \theta_2\mathbf{s}$ lie in $[0,1]$,
- at least one entry of $\mathbf{x}(t) - \theta_2\mathbf{s}$ becomes integer or at least one entry of $A_2(\mathbf{x}(t) - \theta_2\mathbf{s}) - \mathbf{b_2}$ becomes zero.

Finally, the new solution is obtained as follows:

$$\mathbf{x}(t+1) = \begin{cases} \mathbf{x}(t) + \theta_1\mathbf{s}, & \text{with probability } \frac{\theta_2}{\theta_1+\theta_2}, \\ \mathbf{x}(t) - \theta_2\mathbf{s}, & \text{with probability } \frac{\theta_1}{\theta_1+\theta_2}. \end{cases} \tag{8}$$

The three aforementioned guarantees can be verified as follows. Firstly, $E[\mathbf{x}(t+1)] = E[\mathbf{x}(t)]$ will be proved in Lemma IV.3. Secondly, since $\mathbf{s}$ is taken from null space of A_1, we have $A_1\mathbf{s} = \mathbf{0}$, and thus all tight constraints are still tight (e.g., $A_1(\mathbf{x}(t) + \theta_1\mathbf{s}) = A_1\mathbf{x}(t) = \mathbf{b_1}$). Finally, the third guarantee is accomplished through the criteria of choosing θ_1, θ_2 as described above. We can see that the dependent rounding algorithm is able to round at least one fractional variable into a binary value or make at least one untight constraint become tight. Therefore, it rounds all fractional variables into integers with at most N_T iterations, where N_T is the total number of variables and untight constraints.

However, the necessary condition for the success of the rounding algorithm is that the null space of the matrix for tight constraints (i.e., A_1) is nontrivial. If not, some constraints must be dropped or combined, which can result in the violation of these constraints. More importantly, no common procedure exists for dropping or combining constraints to guarantee success of the algorithm. Instead, the criteria of constraint dropping and combining depend on specific problem structures. Next, we propose a dependent rounding algorithm with an efficient constraint dropping procedure for X^*.

Before we present the rounding algorithm, we first prove the following lemma.

Lemma IV.1. *$C2$ of (P.2) will not be violated in the dependent rounding of $x^*_{ij}, \forall(i,j)$, and thus can be removed in the design of the dependent rounding algorithms.*

Proof. Since X^* satisfy all $C1 - C3$ constraints of (P.2), according to $C2$, $C_{ij} = 0$ implies $x^*_{ij} = 0, \forall(i,j)$, and $C_{ij} = 1$ implies $x_{ij} \in [0,1], \forall(i,j)$. Hence, $C2$ constraints (and corresponding variables) can be divided into two parts: $C2_1 = \{(i,j)|C_{ij} = 0\}$, and $C2_2 = \{(i,j)|C_{ij} = 1\}$. Moreover, since the dependent rounding algorithm aims to only round fractional variables $x^*_{ij} \in (0,1)$ into binary values, variables in $C2_1$ will not be changed and variables in $C2_2$ are rounded to at most 1. Therefore, no $C2$ constraints will be violated. ■

Lemma IV.1 shows that we only need to consider constraints in $C1$ and $C3$. For a given set of fractional variables, let F_k denote the subset of vehicles i for which there are exactly k fractional variables $x^*_{ij} \in (0,1)$, i.e., V_i communicates with k neighbors "fractionally". Hence, there can be at most $N-1$ subsets $F_1, F_2, \cdots F_{N-1}$. In addition, let $|F_k|$ be the number of vehicles in F_k. Given these notations, details on the proposed dependent rounding algorithm are shown in Algorithm 1.

Algorithm 1 Dependent Rounding Algorithm for X^*

Input: Fractional communication assignment to (P.2): X^*
Output: Integer V2V communication assignment to (P.2): X
Initialization : $\mathbf{x}(\mathbf{0}) = X^*$

```
while there exist fractional variables in x(t) do
    treat all integer variables in x(t) as constants
    Constraint Dropping:
        (1) for vehicles in F_1, drop all their CRLB constraints;
        (2) if |F_2| > 0, |F_k| = 0, ∀k ≠ 2 and tight CRLB
        constraints of vehicles in F_2 are linearly independent,
        drop one of the tight CRLB constraints randomly
    find the null-space S of new set of tight constraints
    choose a nonzero vector s ∈ S
    find scalars θ_1, θ_2 as described right above Equation (8).
    compute x(t+1) using Equation (8)
end while
return x(t+1)
```

Remainder of this section is focused on the feasibility and optimality analysis of Algorithm 1. Firstly, feasibility of Algorithm 1 is proved in Lemma IV.2.

Lemma IV.2. *In Step 4 of Algorithm 1, the null-space S is always nontrivial.*

Proof. Existence of the nontrivial null space means that current linear system "$A_1(t)\mathbf{x(t)} = \mathbf{b_1}(t)$" defined by all tight constraints of (P.2) is undetermined, i.e., the number of linearly independent equations is less than the number of variables. Hence, we only need to prove that after the constraint dropping in Step 3, the number of linearly independent tight constraints (denoted by N_c) is less than the number of pure fractional variables (denoted by N_v) in every iteration. We prove this lemma using contradiction, i.e., we first suppose $N_v \leq N_c$. Given the definition of subsets $F_1, F_2, \cdots F_{N-1}$, we have

$$N_v = \sum_{k=1}^{N-1} k \times |F_k|. \tag{9}$$

Next, we compute the value of N_c. Since $C2$ constraints have been removed due to Lemma IV.1, the set of tight constraints consists of CRLB constraints (i.e., $C1$ in (P.2)) and assignment constraints (i.e., $C3$ in (P.2)). Let N_{C1} be the number of tight CRLB constraints, and N_{C3} be the number of tight assignment constraints. Since each "fractionally" scheduled vehicle i (i.e., there exists a j such that $x_{ij} \in (0,1)$) has to satisfy its CRLB constraint (not necessarily with equality), we have $N_{C1} \leq \sum_{k=1}^{N-1} |F_k|$. However, according to Step 3, all constraints in F_1 are dropped, and thus $N_{C1} \leq \sum_{k=2}^{N-1} |F_k|$. In addition, since all fractional variables appear in pair in $C3$ constraints, we have $N_{C3} = \frac{N_v}{2}$. Hence, N_c is bounded as follows,

$$N_c \leq N_{C1} + N_{C3} \leq \sum_{k=2}^{N-1} |F_k| + \frac{N_v}{2}, \tag{10}$$

where the first inequality is due to that the tight constraints may not be linearly independent. Then, the assumption $N_v \leq N_c$ implies that $N_v \leq \sum_{k=2}^{N} |F_k| + \frac{N_v}{2}$, i.e.,

$$\frac{1}{2}|F_1| + |F_2| + \sum_{k=3}^{N-1} \frac{k}{2}|F_k| \leq |F_2| + \sum_{k=3}^{N-1} |F_k|. \tag{11}$$

which is satisfied if and only if $|F_2| > 0, |F_k| = 0, \forall k \neq 2$, and $N_c = N_{C1} + N_{C3}$, i.e., all tight constraints are linearly independent. However, according to Step 3, whenever this happens, one of the tight CRLB constraints is dropped, which means that Equation (11) can not be satisfied. Therefore the assumption $N_v \leq N_c$ does not hold, and thus the nontrivial null-space S always exists. ■

Next, optimality analysis of Algorithm 1 is as follows.

Lemma IV.3. *Let $\mathbf{x}(t+1)$ be the integer solution returned by Algorithm 1, then $E[\mathbf{x}(t+1)] = X^*$.*

Proof. According to Step 7, we have

$$\begin{aligned} E[\mathbf{x}(t+1)|\mathbf{x}(t)] &= \frac{\theta_2}{\theta_1+\theta_2}(\mathbf{x}(t) + \theta_1 \mathbf{s}) \\ &+ \frac{\theta_1}{\theta_1+\theta_2}(\mathbf{x}(t) - \theta_2 \mathbf{s}) = \mathbf{x}(t). \end{aligned} \tag{12}$$

Hence, we have

$$E[\mathbf{x}(t+1)] = E[E[\mathbf{x}(t+1)|\mathbf{x}(t)]] = E[\mathbf{x}(t)]. \tag{13}$$

Since $\mathbf{x}(\mathbf{0}) = X^*$ according to "Initialization" of Algorithm 1, we have

$$E[\mathbf{x}(t+1)] = E[\mathbf{x}(t)] = \cdots = E[\mathbf{x}(\mathbf{1})] = \mathbf{x}(\mathbf{0}) = X^*, \tag{14}$$

which finishes the proof. ■

This lemma shows that the optimum of (P.2) is achieved and all constraints are satisfied in expectation. Then, we study how the constraint dropping in Step 3 affects the worst case CRLB constraint violation. Let $CRLB_i, CRLB_i^*$ be the achieved CRLB and required CRLB of V_i respectively, and we show that the violation ratio can be upper bounded as follows.

Lemma IV.4. *Let $a_i = \frac{1+(m_i^*-1)(1-\alpha)}{\sigma_i^2}$, and $\delta_i = \frac{CRLB_i - CRLB_i^*}{CRLB_i^*}$ be the CRLB violation ratio of vehicle i. Then, we have (1) $\delta_i \leq \max_j \frac{a_j}{a_i}$ for vehicles in F_1, and $\delta_i \leq \max_{j,k} \frac{a_j+a_k}{a_i}$ for vehicles in F_2, and (2) at most one vehicle's CRLB constraint can be dropped in F_2.*

Proof. First, let $CRLB_i^* = \frac{1}{\gamma_i}$ and consider the following tight CRLB constraint of vehicle i dropped from F_1,

$$V_i : a_i + a_j x_{ij} + C_i = \gamma_i, \tag{15}$$

where C_i is a constant consisting of rounded variables. Since x_{ij} is rounded into 0 or 1 eventually, we have

$$\frac{CRLB_i}{CRLB_i^*} \leq \frac{\gamma_i}{a_i + C_i} = \frac{a_i + a_j + C_i}{a_i + C_i} \leq 1 + \max_j \frac{a_j}{a_i}, \tag{16}$$

and thus $\delta_i = \frac{CRLB_i - CRLB_i^*}{CRLB_i^*} \leq \max_j \frac{a_j}{a_i}$.

Similarly, consider the following CRLB constraint of vehicle i dropped from F_2,

$$V_i : a_i + a_j x_{ij} + a_k x_{ik} + C_i = \gamma_i. \tag{17}$$

Then, we have

$$\frac{CRLB_i}{CRLB_i^*} \leq 1 + \max_{j,k} \frac{a_j + a_k}{a_i}, \tag{18}$$

and thus $\delta_i = \frac{CRLB_i - CRLB_i^*}{CRLB_i^*} \leq \max_{j,k} \frac{a_j+a_k}{a_i}$.

Next, we prove the second part of this lemma. According to the proof of Lemma IV.2, both the number of variables and constraints are $|F_2| + N_v/2 = 2|F_2|$ in this scenario. Furthermore, in (P.2), we can merge $C3$ constraints into $C1$ constraints by replacing $x_{ji}, \forall j > i$ with x_{ij}, and end up with a linear system with $|F_2|$ linearly independent constraints and $|F_2|$ fractional variables. In this case, the linear system defined by constraints in F_2 is determined. However, after one constraint

$$V_{i^*} : a_{i^*} + a_{i^*} x_{i^* j_1^*} + a_{i^*} x_{i^* j_2^*} + C_{i^*} = \gamma_{i^*} \tag{19}$$

is dropped, the system becomes undetermined. To show that at most one CRLB constraint is dropped in F_2, we show that this scenario will no longer happen in the remaining iterations.

In general, each fractional x_{ij} appears in two CRLB constraints in F_2: V_i and V_j. Hence, whenever one fractional variable is rounded into an integer, its two corresponding constraints reduce to F_1, and thus are dropped. Hence, the number of remaining constraints will always be less than the number of remaining fractional variables. However, the relationship

between rounded variables and the dropped constraint must be explicitly studied to determine the number of constraints to be dropped. Specifically, we prove the second part of this lemma by considering the following two cases:

Case 1: Only one variable is rounded into an integer. Let x_{ij} be the rounded variable, and we consider the number of constraints to be dropped in the following three sub-cases:

1) $x_{ij} \in \{x_{i^*j_1^*}, x_{i^*j_2^*}\}$. For example, $x_{ij} = x_{i^*j_1^*}$. Since constraint V_{i^*} in Equation (19) has been dropped, only one more constraint $V_{j_1^*}$ will be dropped.
2) $x_{ij} \in \{x_{j_1^*i_1}, x_{i_2j_2^*}\}$, where $x_{j_1^*i_1}$ denotes the other fractional variable apart from $x_{j_1^*i^*}$ in constraint V_{j_1}, and $x_{i_2j_2^*}$ is defined similarly. For example, let $x_{ij} = x_{j_1^*i_1}$. In this case, two constraints $V_{j_1^*}$ and V_{i_1} are dropped.
3) $x_{ij} \notin \{x_{i^*j_1^*}, x_{i^*j_2^*}, x_{j_1^*i_1}, x_{i_2j_2^*}\}$. In this case, two constraints V_i, V_j are dropped after x_{ij} is rounded.

Therefore, in Case 1, at least one CRLB constraint is dropped after one variable is rounded.

Case 2: More than one variables are rounded into integers. Let l be the number of fractional variables and q be the number of dropped constraints. Therefore, we need to prove that $q \geq l$. In addition, let $W = W_1 \cup W_2 = \{V_i | x_{ij} | x_{ji} \in (0,1), \exists j\}$ be the set of all fractionally assigned vehicles, in which $W_1 = \{V_{i^*}, V_{j_1^*}, V_{j_2^*}\}$ is the set of vehicles appearing in the dropped constraint in Equation (19) and W_2 denotes the other vehicles. Next, let W_l denote the set of vehicles appearing in the rounded fractional variables, and we determine the number of additional constraints to be dropped by considering the following two sub-cases:

1) $W_l \cap W_1 = \emptyset$. In this case, the number of involved vehicles is $2l$. Since each involved vehicle in W_2 can appear in at most two constraints, we have
$$q \geq \frac{2l}{2} = l. \tag{20}$$
2) $W_l \cap W_1 \neq \emptyset$. Let $p = |W_l \cap W_1|$, and $p \geq 1$. Since vehicles in W_1 can appear in at most one CRLB constraint while vehicles in W_2 can appear in at most two CRLB constraints, we have
$$q \geq p + \frac{2l - p}{2} = l + \frac{p}{2} > l. \tag{21}$$

Therefore, the number of dropped CRLB constraints is always larger than or equal to the number of rounded variables in remaining iterations. Therefore, after this iteration, the linear system is always undetermined, which finishes the proof. ■

B. Rounding Algorithm for $\mathbf{m}^*$

Since we want to find an integer solution close to the optimal fractional solution, we only consider rounding up (i.e., $m_i = \lceil m_i^* \rceil$) or down (i.e., $m_i = \lfloor m_i^* \rfloor$) of m_i^*. In particular, we simply take advantage of the independent rounding method, i.e., each m_i value is rounded up or down independently from the rounding of other m_j values. Specifically, let $\delta_i = m_i^* - \lfloor m_i^* \rfloor$ be the fractional part of m_i^*, and m_i^* is rounded up with probability δ_i and rounded down with probability $1 - \delta_i$. The performance of the independent rounding is shown in the following lemma.

Lemma IV.5. *Let m_i be the integer value rounded independently from m_i^*, then $E[m_i] = m_i^*$.*

Proof. Since $m_i = \lceil m_i^* \rceil$ with probability δ_i and $m_i = \lfloor m_i^* \rfloor$ with probability $1 - \delta_i$, we have
$$\begin{aligned} E[m_i] &= (m_i^* - \delta_i) \times (1 - \delta_i) + (m_i^* + 1 - \delta_i) \times \delta_i \\ &= m_i^*, \end{aligned} \tag{22}$$
which finishes the proof. ■

C. Optimality and Complexity Analysis

The fractional solutions X^* and $\mathbf{m}^*$ obtained from the QP problem have been rounded using dependent and independent rounding, respectively. Moreover, expectations of the final integer solutions X and $\mathbf{m}$ are both guaranteed to be equal to their original fractional values (see Lemma IV.3 and IV.5). Moreover, since the rounding of $\mathbf{m}^*$ is independent of X, all quadratic items in (P.2) satisfy $E[m_i^* x_{ij}^*] = E[m_i^*] \times E[x_{ij}^*]$. Therefore, the QP-based method is optimal in expectation.

Recall that the number of iterations of Algorithm 1 is proportional to the total number of variables and constraints, that is $O(N_v + N_c) = O\left(N(N-1) + N + \frac{N(N-1)}{2}\right) = O(N^2)$. Moreover, finding null-space of a matrix takes at most $O(N^3)$ time. Thus, the complexity of rounding X^* is at most $O(N^5)$. The complexity of rounding $\mathbf{m}^*$ is simply $O(N)$. Hence, the total complexity of the algorithm is at most $O(N^5)$.

V. Numerical Results

In this section, we study performance of the proposed method through simulations in MATLAB. Specifically, we consider a mobile vehicular network with N vehicles, where $N \in \{5, 7, 10, 12, 15, 17, 20, 22, 25\}$.

A. Simulation Setup

In the following simulations, we set $T_0 = 1, T_i \in [1, 10], \sigma_i^2 \in [1, 6], \forall i$, and consider the three temporal correlation levels: low ($\alpha = 0.2$), medium ($\alpha = 0.5$) and high ($\alpha = 0.7$). Links in the radar band require line-of-sight paths between transmitter and receiver. In our numerical evaluations, we assume that only half of the vehicle pairs can establish line-of-sight links and the remaining links are assigned zero capacity, i.e., $C_{ij} = 0$ in (P.1). Performance of the proposed algorithm is evaluated from three perspectives: remaining time ratio, expected and the worst case CRLB violation.

B. Simulation Results

Let "QP" and "RD" be the fractional solution to quadratic program of (P.2) and the integer solution returned by our algorithm, respectively. Recall that "QP" is an upper bound of the optimal integer solution to (P.2) because it is obtained by relaxing all integer constraints of (P.2). Moreover, we can see from Figure (4a) that the expected value of "RD" is almost identical to "QP", which verifies our algorithm is optimal in expectation.

Figure (4a) also shows that the remaining time ratio first increases with increasing N, and converges eventually. The reason is that several vehicles with less estimation errors

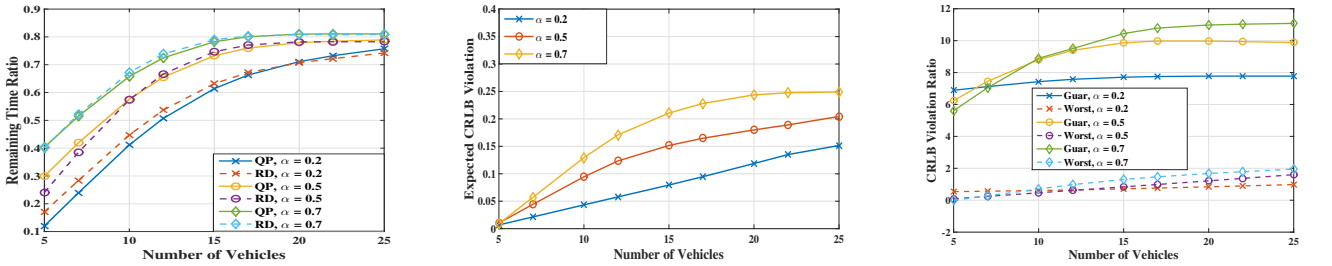

(a) Left Time Ratio for Other Communications (b) Expected CRLB Violation Ratio (c) Worst CRLB Violation and its Upper Bound

Figure 4. Performance of the proposed spectrum resource allocation algorithm

can achieve high accuracy imaging results and most other vehicles can achieve CRLB requirements by communicating with these vehicles. Thus the remaining time ratio increases with increasing N. Moreover, the scheduling period T also increases (with a maximum limit) with increasing N in the pure automotive radar network. Hence, total radar imaging time, time for exchanging imaging results, and T all become proportional to N eventually. Therefore, the remaining time ratio for other communications converges.

For example, suppose two vehicles have very low estimation errors, and they can achieve CRLB requirements by transmitting multiple radar pulses. Since transmitting M_i pulses already guarantees they achieve CRLB requirements, and they will further improve imaging accuracy through communications, they only need to transmit M_i pulses. In this case, other vehicles only transmit one radar pulse and achieve CRLB requirements through exchanging imaging results with the two vehicles. Let T_b be the time allocated to each new vehicle in the pure automotive radar network, and T_1 be the round-trip-time between all other vehicles and the target. As shown in Figure 3, we have $T_R = 2 \times T_b + (N-2) \times T_1$. Next, we compute the total time for exchanging imaging results (i.e., T_C in Figure 3). Firstly, the two vehicles transmit their imaging results to other vehicles, which takes $(N-2)\times(M_1+M_2)\times T_0$ time. Then, other vehicles transmit their imaging results to the two vehicles, which takes $(N-2)\times 2\times 1\times T_0$ time. Hence, we have $T_C = (N-2)(M_1+M_2+2)T_0$, and the total time ratio for radar imaging and exchanging results (i.e., $\frac{T_R+T_C}{T}$) converges to $\frac{T_1+(M_1+M_2+2)T_0}{T_b}$ for sufficiently large N. Therefore, the left time ratio also converges.

Figures (4b) and (4c) show that both the expected and worst case CRLB violations increase with increasing N, which can be explained using Lemma IV.4. Specifically, Lemma IV.4 implies that violation ratio in the whole JARC network is bounded by $\frac{\max_{j,k\in S} a_j+a_k}{\min_{i\in S} a_i}$, where S denotes the set of all fractionally assigned vehicles. Hence, CRLB violation increases with growing S, i.e., increasing N. Moreover, CRLB violation ratio converges because a_i values are bounded. Specifically, Lemma IV.4 shows that a_i is determined by m_i and σ_i. In the simulation setup, σ_i is bounded between $[1, 6]$, m_i values are bounded as explained in the previous paragraph.

Figure 4 shows that both left time ratio and CRLB violations increase with increasing α. The reason is that increasing correlation level means it's less efficient to achieve CRLB requirements via radar detection. Thus more vehicles achieve CRLB requirements through communications, which leaves more time for other communications. Moreover, S also grows with N, and thus CRLB violation increases as explained in the previous paragraph. Finally, we can see that Figure 4 verifies that our proposed algorithm is optimal in expectation and satisfies the constraint violation bounds in Lemma IV.4.

VI. Conclusion

In this paper, we present a theoretical study of the JARC network. Firstly, we study the tradeoff between RI operations and V2V communications using estimation theory. Then, we formulate the resource allocation problem to be an integer quadratic program. Finally, we propose a QP-based method, which achieves optimal (in expectation) remaining time ratio at the cost of bounded CRLB violations. One of our future works is to develop distributed algorithms with more favorable implementation characteristics.

References

[1] M. Hassan, H. Vu, and T. Sakurai, "Performance analysis of the IEEE 802.11 MAC protocol for DSRC safety applications," *Vehicular Technology, IEEE Transactions on*, vol. 60, no. 8, pp. 3882–3896, 2011.

[2] V. Winkler, J. Detlefsen, U. Siart, J. Buchler, and M. Wagner, "Automotive radar sensor with communication capability," in *Wireless Technology, 2004. 7th European Conference on*, Oct 2004, pp. 305–308.

[3] L. Han and K. Wu, "24-GHz integrated radio and radar system capable of time-agile wireless communication and sensing," *Microwave Theory and Techniques, IEEE Transactions on*, vol. 60, no. 3, pp. 619–631, 2012.

[4] H. L. V. Trees, *Detection, Estimation, and Modulation Theory: Radar-Sonar Signal Processing and Gaussian Signals in Noise*. Melbourne, FL, USA: Krieger Publishing Co., Inc., 1992.

[5] R. Raup, R. Ford, G. Krumpholz, M. Czerwinski, and T. Clark, "The best approximation of radar signal amplitude and delay," *The Lincoln Laboratory Journal*, vol. 3, no. 2, pp. 3882–3896, 1990.

[6] M. Rockl, T. Strang, and M. Kranz, "V2V communications in automotive multi-sensor multi-target tracking," in *Vehicular Technology Conference, 2008. VTC 2008-Fall. IEEE 68th*, Sept 2008, pp. 1–5.

[7] F. Baselice, G. Ferraioli, G. Matuozzo, V. Pascazio, and G. Schirinzi, "3D automotive imaging radar for transportation systems monitoring," in *Environmental Energy and Structural Monitoring Systems (EESMS), 2014 IEEE Workshop on*, Sept 2014, pp. 1–5.

[8] M. McDonnell, H. Possingham, I. Ball, and E. Cousins, "Mathematical methods for spatially cohesive reserve design," *Environmental Modeling & Assessment*, vol. 7, no. 2, pp. 107–114, 2002.

[9] B. Saha, "Approximation algorithms for resource allocation," Ph.D. dissertation, University of Maryland, College Park, Department of Computer Science, 2011.